Supplementary Materials

Supplementary Materials S1. Relevant characteristics of climate stations used for the SWAT model. Stations listed from low to high elevation above sea level.

Station	Latitude (° N)	Longitude (° W)	Elevation (masl)	Data[1]	Period used	Use[2]
Aeropuerto Simón Bolivar	11.128	−74.229	4	T_{yrmean}	1952–2016	TLR
Prado Sevilla	10.764	−74.155	18	P_d	1970–2013	WeatherGen, Simulation
				T_{dmax}, T_{dmin}	1978–2013	
				RH_m	1968–2013	
				P_{yr}	1980–2013	PLR
				T_{yrmean}	1967–2014	TLR
La Ye	10.992	−74.211	20	P_d	1970–2013	WeatherGen, Simulation
				T_{dmax}, T_{dmin}	1976–2013	
				RH_m	1968–2013	
				T_{yrmean}	1968–2013	TLR
				P_{yr}	1980–2013	PLR
Padelma	10.721	−74.200	20	T_{yrmean}	1967–2016	TLR
				P_{yr}	1980–2013	PLR
El Enano	10.902	−74.189	25	P_d	1975–2016	Simulation
				P_{yr}	1980–2013	PLR
La Esperanza	10.742	−74.306	25	P_{yr}	1980–2013	PLR
El Cenizo	10.652	−74.073	450	P_{yr}	1980–2013	PLR
Minca	11.141	−74.120	640	P_{yr}	1980–2013	PLR
San Pablo	10.808	−74.027	800	P_{yr}	1980–2013	PLR
El Palmor	10.773	−74.026	1200	P_d	1976–2016	Simulation
				P_{yr}	1980–2013	PLR
San Pedro de la Sierra	10.900	−74.500	1400	T_{yrmean}	1972–1979	TLR
Vista Nieves	11.085	−74.080	2000	P_d	1974–2016	Simulation
				P_{yr}	1980–2013	PLR
San Lorenzo	11.111	−74.055	2200	P_d	1969–2016	WeatherGen, Simulation
				T_{dmax}, T_{dmin}	1978–2016	
				RH_m	1969–2013	
				T_{yrmean}	1969–2016	TLR
				P_{yr}	1969–2016	PLR

[1] T_{yrmean}: Annual mean temperature, P_{yr}: Annual total precipitation, P_d: Daily total precipitation, T_{dmax}: Daily maximum temperature, T_{dmin}: Daily minimum temperature, RH_m: Monthly mean relative humidity. [2] TLR: Temperature lapse rate, PLR: Precipitation lapse rate, WeatherGen: SWAT Weather generator.

Supplementary Materials S2. SWAT calibration and validation methods

1. Lapse Rates

We estimated precipitation lapse rates from climate stations ranging in elevation from 4 to 2200 masl located within ~25 km of the watershed (Supplementary Materials S1). Calculated lapse rates were assigned as follows: (1) 500 mm/km for subbasin 15 (Figure 1), which had most of its area below 600 masl, (2) 262 mm/km for subbasins with most of their area between 600 and 2000 masl (subbasins 4, 5, 7–12, 14), and (3) zero for subbasins above 2000 masl, since there were no reliable rainfall records at higher elevations (subbasins 1–3, 6, 13). We implemented the above lapse rates by defining elevation bands with an interval of 500 m. We calculated the temperature lapse rate from 6 stations at elevations between 4 and 2200 masl, within a distance of ~25 km from the watershed (Supplementary Materials S1).

2. Pre-processing of Stream Discharge

We screened discharge data for quality flags and presence of outliers (i.e., values 1.5 times the interquartile range above the upper quartile on log-transformed data). Daily records that had a quality flag and were also outliers were excluded from further analysis (i.e., considered as days with missing records). Since model calibration and validation were performed on a monthly basis, daily average discharge values were processed to obtain monthly average discharge. We discarded months that had more than 3 missing daily records.

3. Pre-Processing and Calibration of LAI

Studies show that SWAT´s default algorithm for determining vegetation dormancy versus growth do not provide an adequate representation of the tropics [51,52]. The main reason is that vegetation growth in these regions is triggered by changes in soil moisture rather than by changes in day length. As a result, the use of day-length does not capture tropical ecohydrological processes correctly, even if model performance statistics are within satisfactory ranges [51]. Strauch, Volk and Alemayehu et al. [51,52] introduced modified vegetation growth modules within SWAT to include months that represent the transition between dry and wet seasons, and therefore trigger vegetation growth. We used the modified vegetation growth module SWAT-T [52] and followed the methods in [52] for LAI data processing and definition of SWAT-T parameters. MODIS LAI data for the study period were downloaded and cropped to our study region. Only pixels with the best quality (LAI_QC = 0) were kept for further processing. In order to extract LAI values for different land covers, we processed polygons from the land cover layer in the following way: (i) selected the largest contiguous polygon within the basin for each land cover, (ii) applied an internal buffer of 100–200m in order to reduce the risk of including mixed border pixels, (iii) checked that the buffered polygon had an area of at least 7.5 km^2 (~ 30 LAI pixels). Only three land covers complied with the area requirement, FRST (77 km^2), RNGB (14 km^2) and COFF (9.8 km^2). We therefore considered areas outside of the basin for FRSD (extended polygon area of 59 km^2) and excluded the remaining land covers from this analysis as they either represented minor percentages within the basin (i.e., RNGE and BANA) or had polygons that were either too small or too narrow even when considering neighboring basins (i.e., PAST). For the excluded categories, we either used values found in the literature (RNGE and PAST), or the default SWAT values (BANA). For the other land cover classes, we used the above polygons to extract mean LAI values for each land cover/time period (8-day composite). Periods that had less than 30 valid pixel values were discarded. Invalid pixels values included NoData pixels, or pixels with anomalous values based on literature reviews (e.g., forest LAI pixels with LAI values < 1.0). As noted by [51,52], LAI data had high temporal variability even after quality control efforts, due to inevitable signal noise. We used the Breaks for Additive Seasonal and Trend (BFAST) method [66] available in R to extract LAI´s trend and seasonal components for each land cover. We used this filtered time series as reference to manually calibrate SWAT parameters related to LAI within SUFI-2 (Supplementary Materials S3). SWAT´s LAI for each land cover was calculated as the HRU areaweighted mean for each day. Once LAI calibration was deemed satisfactory based on visual assessment, LAI parameters were fixed prior to subsequent calibration steps.

4. Calibration of Monthly Streamflow

We initially ran one iteration with 1000 simulations using the parameter ranges defined by the sensitivity analyses and the above-mentioned consideration of goals. We selected the Nash-Sutcliffe efficiency as objective function and used it in conjunction with other statistics to evaluate iteration results (e.g., p-factor and r-factor) [45,46]. The p-factor refers to the fraction of the measured data bracketed by the 95PPU band, and ranges from 0 to 1, with 1 indicating that 100% of the measured data are within the model prediction uncertainty. The r-factor is indicative of the 95PPU width and is calculated as the ratio of the average width of the 95PPU band and the standard deviation of the measured variable, with ideal values close to 0. We also assessed iteration results by comparing average water flux components with the reference values mentioned above. We ran further iterations using SUFI-2 suggested parameter ranges, unless they were outside reasonable values, in which case we modified them manually. We ran subsequent simulations in an iterative manner until we reached satisfactory results. Modifications introduced during the iterative process included alternative watershed setups (e.g., configuration of subbasins and elevation bands), variations to the parameter ranges, and addition of other parameters not selected by the sensitivity analyses but that had a desired effect on water flux components. An example of the latter was the maximum canopy storage parameter (CANMX), which was found to have an effect on the surface runoff component, and was therefore set to values within the range found in the literature for forest and coffee [67,68 and references therein]. After such modifications, sensitivity and calibration analyses were repeated.

Supplementary Materials S3. SWAT parameters used for LAI calibration. Parameters LAI_INIT, BIO_INIT and PHU_PLT are required when the land cover status code (IGRO) is set to 1, indicating that vegetation is already growing at the beginning of the simulation.

Parameter	Description	Calibrated value [1]					
		FRST	FRSD	RNGB	COFF	PAST	RNGE
LAI_INIT	Initial leaf area index (m^2/m^2)	5*	3.8*	6.3*	6*	3 [69]	2.5 [70]
BIO_INIT	Initial dry weight biomass (kg/ha)	50,000 [71]	15,000 [72–74]	10,000 [75]	23,000 [76,77]	3000 [78]	20,000 [79]
PHU_PLT[2]	Total number of heat units or growing degree days needed to bring plant to maturity	4000	4000	4300	5000 [49]	4000	4000
BLAI[3]	Maximum potential leaf area index (m^2/m^2)	7.5* 4.8	11***	9***	7.5* 5.6	4**	2.5**
ALAI_MIN	Minimum leaf area index (m^2/m^2)	3.5*	1*	4.9*	4.6*	0.7 [51]	0.7 [51]
FRGRW1	Fraction of PHU corresponding to the 1st point on the optimal leaf area development curve	0.15***	0.05***	0.01***	0.07***	0.05**	0.05**
FRGRW2	Fraction of PHU corresponding to the 2nd point on the optimal leaf area development curve	0.2***	0.4***	0.07***	0.2***	0.49**	0.25**
LAIMX1	Fraction of BLAI corresponding to the 1st point on the optimal leaf area development curve	0.15***	0.05***	0.1***	0.15***	0.05**	0.1**
LAIMX2	Fraction of BLAI corresponding to the 2nd point on the optimal leaf area development curve	0.99***	0.99***	0.95***	0.99***	0.95**	0.7**
DLAI	Fraction of PHU when LAI begins to decline	0.25***	0.8***	0.7***	0.3***	0.99**	0.35**
T_BASE	Minimum temperature for plant growth (°C)	5***	10**	10***	10 [49]	12**	0**
T_OPT	Optimal temperature for plant growth (°C)	25***	30**	25**	30 [49]	25**	13**
BIO_E	Radiation use efficiency ((kg /ha)/(MJ/m^2))	15**	15**	20***	10**	35**	34**
CHTMX	Maximum canopy height (m)	6**	6**	2***	2**	0.5**	1.0**

SOS1[4]	Dry-wet transition month 1	Defined at the subbasin level[5]: Upper subbasins: 9 (September) Mid subbasins: 11 (November) Lower subbasin: 3 (March)
SOS2[4]	Dry-wet transition month 2	Defined at the subbasin level[5]: Upper subbasins: 10 (October) Mid subbasins: 12 (December) Lower subbasin: 4 (April)

[1] *MODIS, **default SWAT value (for RNGE, T_BASE and T_OPT from SWAT´s cool season plant values), ***manual adjustment during calibration. Number in brackets refers to source in reference list. [2] Values within ranges estimated from local temperature records and other studies in tropical areas [51,52], except for coffee. [3] For MODIS data: Upper value is the maximum LAI value, lower value is the LAI value. [4] SWAT-T parameter estimated from soil moisture index and LAI filtered time series [52]. [5] Subbasins shown in Figure 1. Upper subbasins are subbasins 1, 2, 3, 4, 6, 8, 11, 13. Mid subbasins are subbasins 5, 7, 9, 10, 12, 14. Lower subbasin is subbasin 15.

Supplementary Materials S4. Global sensitivity analysis. Sensitive parameters are indicated by a high t-statistic value (in absolute terms) and a low p-value. Parameters are listed from high to low sensitivity. CANMX values for forest and coffee were set to reference values prior to the sensitivity analysis.

Parameter.	**Description** [1]	**Scaling type**	**Range**		**t-statistic**	**p-value** [2]
			min	max		
CN2	Runoff curve number for moisture condition II	r	−0.25	0.25	−31.654	0.0000
SOL_K	Saturated hydraulic conductivity (mm/hr)	r	−0.5	0.5	−19.265	0.0000
SOL_BD	Moist bulk density (g/cm^3)	r	−0.2	0.2	−11.630	0.0000
ALPHA_BF	Baseflow alpha factor (1/days)	v	0.01	1	−10.748	0.0000
CH_K(2)	Effective hydraulic conductivity in main channel alluvium (mm/hr)	v	0	150	7.643	0.0000
GWQMN	Threshold depth of water in the shallow aquifer required for return flow to occur (mm H_2O)	v	0	5000	-3.668	0.0003
SOL_AWC	Available water capacity of the soil layer (mm H_2O/mm soil)	r	−0.5	0.5	−3.413	0.0007
ESCO	Soil evaporation compensation factor	v	0.01	1	−2.583	0.1008
GW_REVAP	Groundwater revap coefficient	v	0.02	0.2	−2.139	0.0329
SURLAG	Surface runoff lag coefficient	v	0.01	15	1.721	0.0860
SOL_Z	Depth from soil surface to bottom of layer (mm)	r	−0.5	0.5	−1.593	0.1118
EPCO	Plant uptake compensation factor	v	0.01	1	1.208	0.2275
SHALLST	Initial depth of water in the shallow aquifer (mm H_2O)	v	0	1000	1.194	0.2332
REVAPMN	Threshold depth of water in the shallow aquifer for "revap" or percolation to the deep aquifer to occur (mm H_2O)	v	0	1000	0.381	0.7032
GW_DELAY	Groundwater delay time (days)	v	0.01	500	−0.356	0.7220
OV_N	Manning´s "n"value for overland flow	r	−0.3	0.3	0.275	0.7837

[1] From [54]. [2] Parameters with p-values < 0.05 were included in the calibration, except for GW_DELAY which was also included after considering the one-at-a-time sensitivity analysis results.

Supplementary Materials S5. Comparison of SWAT average water flux components prior and after calibration with reference values. Calibration period from 2002 to 2008.

Model	SWAT average water flux components[1] (mm/yr)								Ratios		
	PREC	SURQ	LATQ	GWQ	PET	ET	REVAP	WYLD	Baseflow ratio (GWQ/WYLD)	Runoff ratio (SURQ/WYLD)	ET ratio [(ET+REVAP)/PREC]
Initial	2385.1	548.0	880.7	229.3	1366.9	699.9	27.3	1658.0	0.14	0.23	0.30
Calibrated	2385.1	198.6	779.4	605.6	1366.9	869.9	3.9	1583.7	0.38	0.08	0.37
% change	NA	−63.8	−11.5	164.1	NA	24.3	−85.6	−4.5			
Reference values								1559.0[2]	0.40–0.50[3]	0.04–0.16[4]	~0.40[5]

[1] PREC = precipitation, SURQ = surface runoff contribution to streamflow, LATQ = lateral flow contribution to streamflow, GWQ = groundwater contribution to streamflow, PET = potential evapotranspiration, ET = actual evapotranspiration, REVAP = amount of water moving from shallow aquifer to plants/soil profile, WYLD = water yield. [2] Observed discharge records from IDEAM. [3] From baseflow filter (https://engineering.purdue.edu/mapserve/WHAT/) [4] Runoff measured under different coffee growing systems (lowest value in shade grown coffee, highest value in sun grown coffee) in the central Colombian Andes [49]. [5] 37% for soil with short cover crop in the coffee growing region of Colombia [48], 50-60% for different land covers in the central Colombian Andes [50].

Supplementary Materials S6. Parameter ranges and best-fit parameter value for the selected SWAT model. Scaling type: v (absolute) indicates that the parameter is replaced by the given value, r (relative) indicates that the parameter is multiplied by [1 + (given value)]. The latter preserves the parameter´s spatial variability.

Parameter	**Description**	**Scaling type**	**Range**		**Best-fit parameter value**
			min	max	
CN2	Runoff curve number for moisture condition II	r	−0.25	0	−0.24
SOL_AWC	Available water capacity of the soil layer (mm H_2O/mm soil)	r	−0.5	0	−0.23
SOL_K	Saturated hydraulic conductivity (mm/hr)	r	−0.5	0	−0.49
SOL_BD	Moist bulk density (g/cm^3)	r	−0.2	0.1	−0.05
ALPHA_BF	Baseflow alpha factor (1/days)	v	0.01	0.2	0.10
GW_REVAP	Groundwater revap coefficient	v	0.02	0.14	0.07
GW_DELAY	Groundwater delay time (days)	v	83	417	127
GWQMN	Threshold depth of water in the shallow aquifer required for return flow to occur (mm H_2O)	v	0	500	255.75
ESCO	Soil evaporation compensation factor	v	0.01	0.2	0.08
CH_K(2)	Effective hydraulic conductivity in main channel alluvium (mm/hr)	v	25	125	37.25

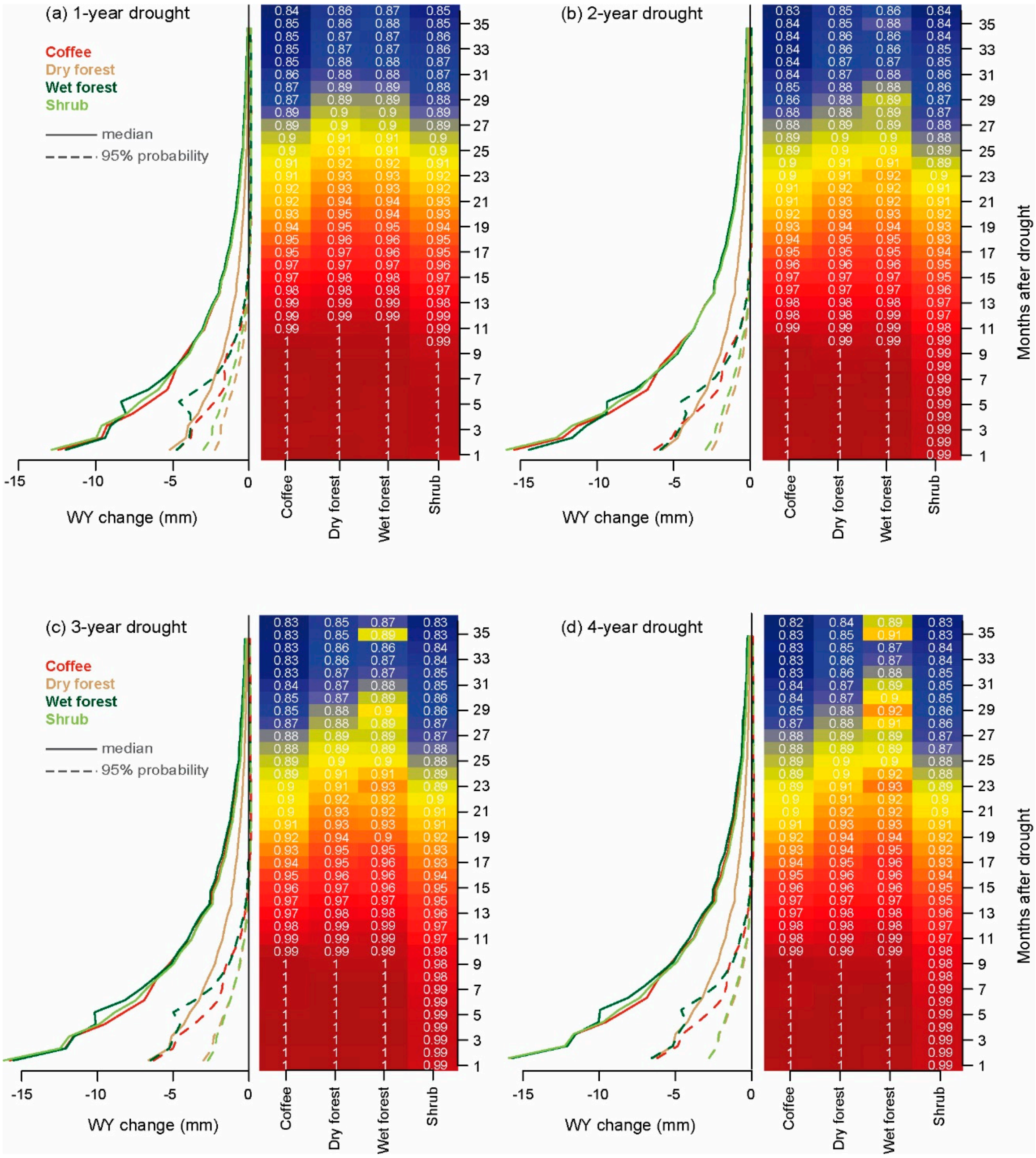

Supplementary Materials S7. Effect of (**a**) 1-year, (**b**) 2-year, (**c**) 3-year, and (**d**) 4-year meteorological drought on water yield (WY) (mm/month) for selected HRUs representative of the study area. For each figure, the left panel shows the median (continuous line) and 95% probability (minimum value, dashed line) of water yield decrease from month 1 through month 36 after drought termination. The vertical line at zero represents no change relative to the reference scenario. Water yield decrease values to the right of the 95% probability line are unlikely. The right panel shows probabilities of water yield decrease with colors scaled from higher (red) to lower (blue) probability.

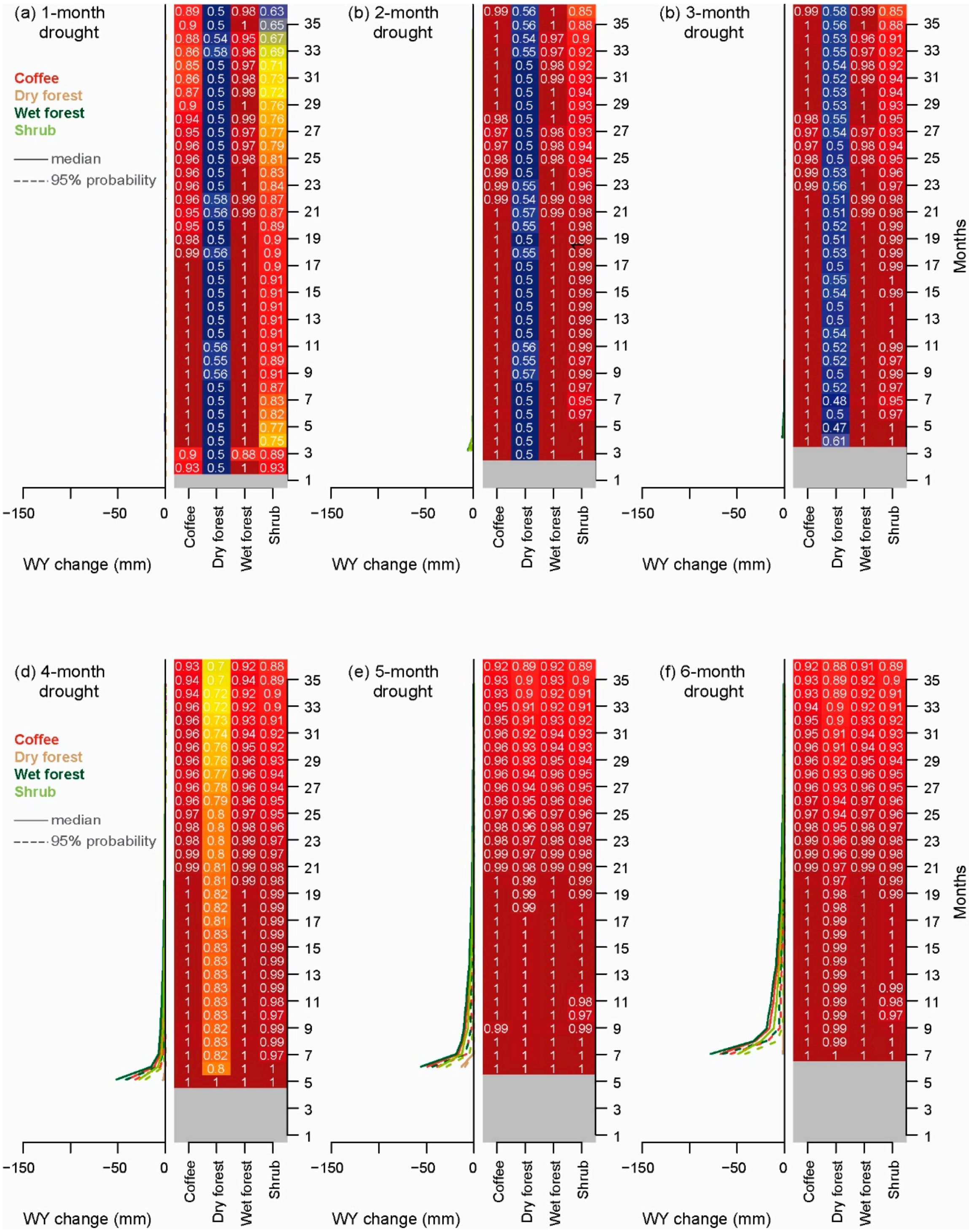

Supplementary Materials S8. Effect of monthly meteorological droughts on water yield (WY) (mm month^{-1}) for selected HRUs representative of the study area. For each figure, the left panel shows the median (continuous line) and 95% probability (dashed line) water yield decrease for subsequent months after drought termination. The vertical line at zero represents no change relative to the reference scenario. Water yield decrease values to the right of the 95% probability line are unlikely. The right panel shows probabilities of water yield decrease with colors scaled from high (red) to low (blue) probability.

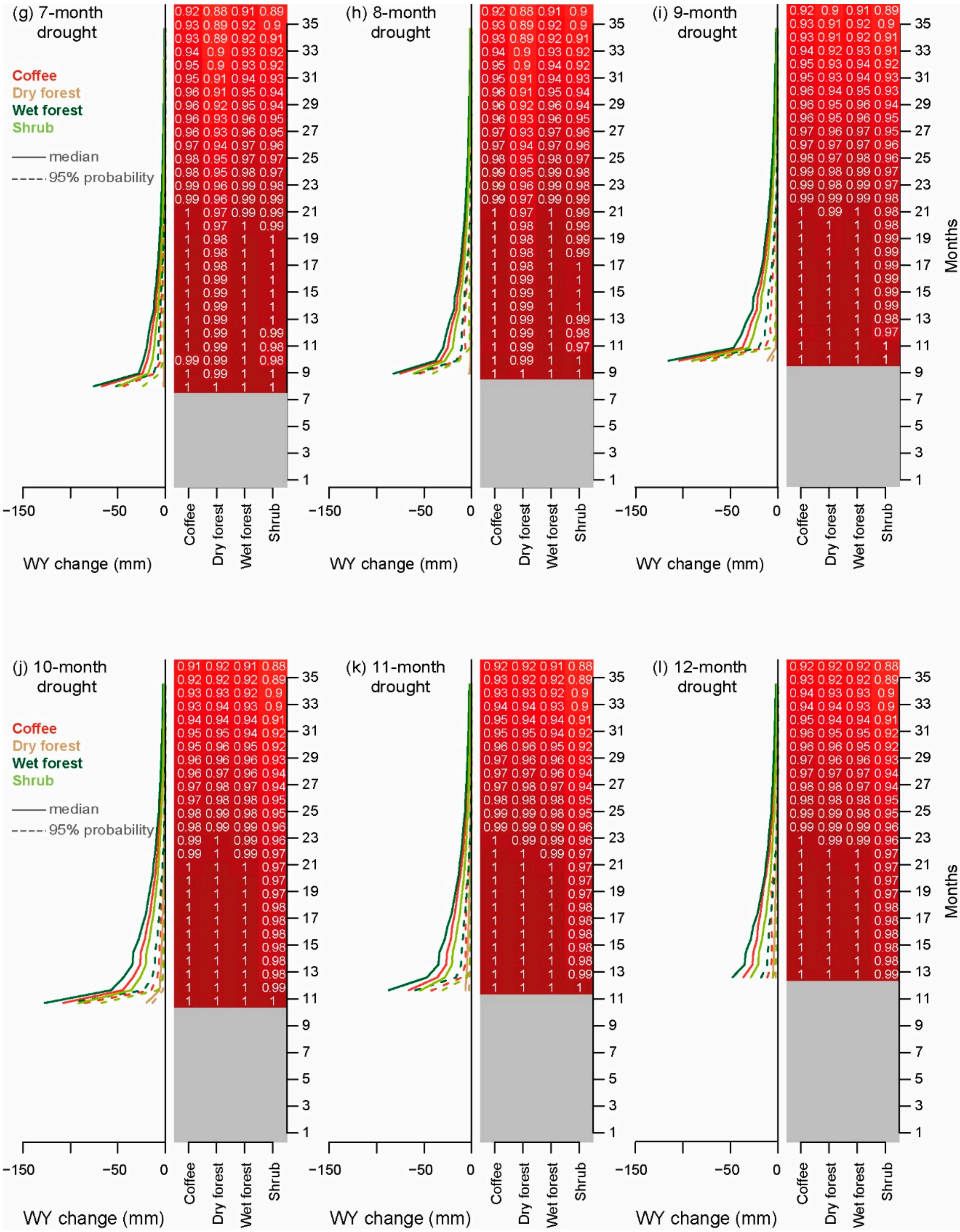

Supplementary Materials S8. (continued).

References

1. Verbesselt, J.; Hyndman, R.; Newnham, G.; Culvenor, D. Detecting trend and seasonal changes in satellite image time series. *Remote Sens. Environ.* **2010**, *114*, 106–115.
2. Jaramillo-Robledo, A. La lluvia y el transporte de nutrimentos dentro de ecosistemas de bosques y cafetales. *Cenicafé* **2003**, *54*, 134–144.
3. Fleischbein, K.; Wilcke, W.; Goller, R.; Boy, J.; Valarezo, C.; Zech, W.; Knoblich, K. Rainfall interception in a lower montane forest in Ecuador: Effects of canopy properties. *Hydrol. Process.* **2005**, *19*, 1355–1371, doi:10.1002/hyp.5562.
4. Rincón, A.; Ligarreto, G.A.; Sanjuanelo, D. Crecimiento del maíz y los pastos (Brachiaria sp.) establecidos en monocultivo y asociados en suelos ácidos del piedemonte llanero colombiano. *Agron. Colomb.* **2007**, *25*, 264–272.
5. Tol, G.J.; Cleef, A.M. Above-ground biomass structure of a Chusquea tessellata bamboo páramo, Chingaza National Park, Cordillera Oriental, Colombia. *Vegetatio* **1994**, *115*, 29–39.
6. Sierra, C.A.; del Valle, J.I.; Orrego, S.A.; Moreno, F.H.; Harmon, M.E.; Zapata, M.; Colorado, G.J.; Herrera, M.A.; Lara, W.; Restrepo, D.E.; et al. Total carbon stocks in a tropical forest landscape of the Porce region, Colombia. *For. Ecol. Manag.* **2007**, *243*, 299–309, doi:10.1016/j.foreco.2007.03.026.
7. Murphy, P.G.; Lugo, A.E. Structure and Biomass of a Subtropical Dry Forest in Puerto Rico. *Biotropica* **1986**, *18*, 89–96, doi:10.2307/2388750.
8. Brandeis, T.J.; del R. Suarez Rozo, M. Effects of model choice and forest structure on inventory-based estimations of Puerto Rican forest biomass. *Caribb. J. Sci.* **2005**, *41*, 250–268.
9. Alvarez, E.; Duque, A.; Saldarriaga, J.; Cabrera, K.; de las Salas, G.; del Valle, I.; Lema, A.; Moreno, F.; Orrego, S.; Rodríguez, L. Tree above-ground biomass allometries for carbon stocks estimation in the natural forests of Colombia. *For. Ecol. Manag.* **2012**, *267*, 297–308, doi:10.1016/j.foreco.2011.12.013.
10. Spracklen, D.V.; Righelato, R. Carbon storage and sequestration of re-growing montane forests in southern Ecuador. *For. Ecol. Manag.* **2016**, *364*, 139–144, doi:10.1016/j.foreco.2016.01.001.
11. Segura, M.; Kanninen, M.; Suárez, D. Allometric models for estimating aboveground biomass of shade trees and coffee bushes grown together. *Agroforest. Syst.* **2006**, *68*, 143–150.
12. Farfán, F.; Sánchez, P.M. Densidad de siembra del café variedad Castillo en sistemas agroforestales, en el Departamento de Santander-Colombia. *Cenicafé* **2016**, *67*, 55–62.
13. Peters, M.; Franco, L.H.; Schmidt, A.; Hincapie, B. *Especies Forrajeras Multipropósito: Opciones para Productores del Trópico Americano*; Centro Internacional de Agricultura Tropical (CIAT): Cali, Colombia, 2011; p. 212.
14. Hofstede, R.G.M.; Mondragón Castillo, M.X.; Rocha Osorio, C.M. Biomass of grazed, burned, and undisturbed páramo grasslands, Colombia. I. Aboveground vegetation. Art. Alp. Res. 1995, 27, 1–12, doi:10.1080/00040851.1995.12003091.